Suppression of IEEE 802.11a Interference in TH-UWB Systems Using Singular Value Decomposition in Wireless Multipath Channels

Shaoyi Xu and Kyung Sup Kwak

Abstract: **Narrow-band interference (NBI) from the coexisting narrow-band services affects the performance of ultra wideband (UWB) systems considerably due to the high power of these narrow-band signals with respect to the UWB signals. Specifically, IEEE 802.11a systems which operate around 5 GHz and overlap the band of UWB signals may interfere with UWB systems significantly. In this paper, we suggest a novel NBI suppression technique based on singular value decomposition (SVD) algorithm in time hopping UWB (TH-UWB) systems. SVD is used to approximate the interference which then is subtracted from the received signals. The algorithm precision and closed-form bit error rate (BER) expression are derived in the wireless multipath channel. Comparing with the conventional suppression methods such as a notch filter and a RAKE receiver, the proposed method is simple and robust and especially suitable for UWB systems.**

Index Terms: **Narrow-band interference (NBI), pulse amplitude modulation (PAM), pulse position modulation (PPM), singular value decomposition (SVD) and maximal ratio combining partial RAKE (MRC PRAKE) receiver, time hopping ultra wideband system (TH-UWB system).**

I. INTRODUCTION

Using trains of sub-nanosecond pulses to convey information, ultra wideband (UWB) technology is a strong candidate for short-rang indoor radio communication systems receiving great attention. The federal communications commission (FCC) currently restricts UWB communication devices to operate under Part 15 rules within the frequency 3.1–10.6 GHz with the emission limit of –41 dBm/MHz [1]. This specification effectively reduces the potential of UWB to interfere with other narrow-band radio technologies making UWB signals cause very little interference with existing narrow-band systems [2]. Nevertheless, due to the low energy per pulse, UWB systems are susceptible to these high-level narrow-band interference (NBI) even though UWB systems may enjoy a high spreading gain due to the large bandwidth. Specifically, IEEE 802.11a systems operate around 5 GHz, which overlap the band of UWB signals regulated by the FCC, and will bring significant interference to UWB systems [3]. If such interference is not suppressed properly, the UWB receiver will be jammed.

Manuscript received July 30, 2006; approved for publication by Jinho Choi, Division II Editor, October 20, 2007.

The authors are with the UWB-ITRC, the Graduate School of Information Technology and Telecommunications, Inha University, 253, Yonghyun-dong, Nam-gu, Incheon, 402-751, Korea, email: shaoyixu@hotmail.com, kskwak@inha.ac.kr.

This research was supported by University IT Research Center Project of Inha UWB-ITRC, Korea.

Some approaches to suppress NBI for UWB systems have been presented. By modeling NBI as a single carrier BPSK modulated waveform, in [4], [5], a technique which consists of selecting the first strongest multipath components and combining them using a RAKE receiver based on the minimum mean square error (MMSE) criterion for TH-UWB systems has been proposed. In [6], the in-band interference is modeled as a cosinusoidal tone and a frequency domain processing combined with a time domain suppression technique for TH-PPM UWB systems is introduced. In [7], a transversal filter with two-sided taps which uses future samples as well as previous samples to reduce the NBI is presented. Additionally, an interference suppression scheme by using multiple receive antennas is examined in [8] and by carefully designing a special pulse is presented in [9].

Although these techniques are effective to suppress single NBI, the NBI suppression technique is still an eminent challenge since the proposed solutions either have high complexity requirements of UWB receivers or are ineffective against strong NBI [10]. Furthermore, surprisingly, the interference suppression technique on IEEE 802.11a systems has received very little attention so far. With the bandwidth as large as several hundred MHz, IEEE 802.11a interference may not be modeled as a BPSK modulated signal or as a cosinusoidal tone. Hereby, many proposed methods seem to be infeasible to suppress IEEE 802.11a interference. Recently, both analytically and empirically, IEEE 802.11a signal was demonstrated to be modeled as bandlimited additive white Gaussian noise [11], [12].

In general, three kinds of UWB concepts have been proposed, namely the multiband orthogonal frequency division multiplexing (MB-OFDM) approach, the time-hopping UWB (TH-UWB) system, and the direct-sequence UWB (DS-UWB) system. The data modulation schemes most often used in UWB systems are pulse amplitude modulation (PAM) and pulse position modulation (PPM). In our work, a novel technique based on singular value decomposition (SVD) algorithm to suppress IEEE 802.11a signals for TH-UWB systems is provided. SVD algorithm is used to estimate NBI which then is subtracted from the received signals. This work is an extension of our previous work [13] to deal with wireless multipath channel case in TH-UWB systems and also includes the conventional notch filter and the maximal ratio combining partial RAKE (MRC PRAKE) receiver for comparison. The algorithm precision and calculation complexity are studied and the closed-form bit error rate (BER) expression is derived for TH-PAM and TH-PPM in indoor multipath environments. Simulation results confirm that our method can suppress NBI effectively and robustly.

The reminder of this paper is organized as follows. In Sec-

tion II, TH-PAM, TH-PPM UWB system models and the IEEE 802.11a signals are described. Section III proposes the SVD algorithm and the NBI suppression scheme. The algorithm estimation precision and performance analysis are derived in Section IV. In Section V, simulation results and some remarks will be presented, followed by a conclusion in Section VI.

II. SYSTEM MODEL

A. UWB System Model

In this paper, we consider the single-user TH-UWB system model modulated by binary pulse amplitude modulation (BPAM) and binary pulse position modulation (BPPM). A TH-BPAM UWB signal takes the form

$$s_{\mathrm{PAM}}(t) = \sum_{j=iN_s}^{(i+1)N_s-1} d_i w_{tr}(t - jT_f - C_jT_c) \tag{1}$$

and a TH-BPPM UWB signal can be expressed as

$$s_{\mathrm{PPM}}(t) = \sum_{j=iN_s}^{(i+1)N_s-1} w_{tr}(t - jT_f - C_jT_c - \delta d_i). \tag{2}$$

Where $s(t)$ is the transmitted UWB signal conveying the ith information bit and w_{tr} is the transmitted signal pulse with a pulse width T_p. T_f denotes a frame duration with $T_f \gg T_p$ to avoid introducing intersymbol interference (ISI). $C_j = C_{j+mN_p}, m = 0, 1, 2, \cdots$ is the jth code of PN sequence with the period N_p, where $0 < C_j \leq N_h$ and N_h is an integer. T_c represents a time-shift unit incurred by the PN sequence and N_s is the number of pulses required to transmit a single information bit. $d_i \in \{\pm 1\}$ in TH-BPAM systems and $d_i \in \{0, 1\}$ for TH-BPPM systems represents the ith transmitted information bit. δ is referred to as a modulation index which is a time-shift unit incurred by the data symbol d_i in TH-BPPM systems.

B. Channel Model and Received Signal

Let $h(t) = \sum_{l=0}^{L-1} \alpha_l \delta(t - \tau_l)$ denote the multipath channel with L paths where α_l and τ_l are the channel attenuation and the channel delay associated with the lth multipath so that the received signal in these two systems can be expressed as

$$\begin{aligned} r_{\mathrm{PAM}}(t) &= s_{\mathrm{PAM}} \otimes h(t) \\ &= \sum_{j=iN_s}^{(i+1)N_s-1} \sum_{l=0}^{L-1} \alpha_l d_i w_{rx}(t - jT_f - C_jT_c - \tau_l) \\ &\quad + i(t) + n(t) \end{aligned} \tag{3}$$

and

$$\begin{aligned} r_{\mathrm{PPM}}(t) &= s_{\mathrm{PPM}} \otimes h(t) \\ &= \sum_{j=iN_s}^{(i+1)N_s-1} \sum_{l=0}^{L-1} \alpha_l w_{rx}(t - jT_f - C_jT_c - \delta d_i - \tau_l) \\ &\quad + i(t) + n(t) \end{aligned} \tag{4}$$

where $\otimes$ denotes the convolution operator and w_{rx} is the received pulse at the output of the antenna. $i(t)$ is the NBI signal and $n(t)$ is the additive white Gaussian noise (AWGN) with two-sided power spectral density (PSD) $N_0/2$. Defining $\boldsymbol{\alpha} = [\alpha_0, \alpha_1, \cdots, \alpha_{L-1}]^T$ and $\boldsymbol{\tau} = [\tau_0, \tau_1, \cdots, \tau_{L-1}]^T$ as the channel attenuation vector and the channel delay vector, respectively and $[\cdot]^T$ denotes transpose. For the purposes of analysis, we assume that τ_l and w_{rx} are known to the receiver. To collect multipath energy, a RAKE receiver is always adopted in UWB systems. The template waveforms of the kth frame for the lth correlator with a time delay τ_l for these two UWB systems are given by

$$\phi^l_{\mathrm{PAM}}(t) = w_{rx}(t - jT_f - C_jT_c - \tau_l) \tag{5}$$

and

$$\begin{aligned} \phi^l_{\mathrm{PPM}}(t) &= w_{rx}(t - jT_f - C_jT_c - \tau_l) - \\ &\quad w_{rx}(t - jT_f - C_jT_c - \delta - \tau_l) \end{aligned} \tag{6}$$

producing the output of the lth correlator

$$r_l(t) = \sum_{j=0}^{N_s-1} \int_{(j-1)T_f}^{jT_f} r(t)\phi^l(t)dt \tag{7}$$

which can be denoted by a vector as $\mathbf{r} = [r_0, r_1, \cdots, r_{L-1}]^T$.

In the present paper, we employ a maximal ratio combining partial RAKE receiver which uses first L_p paths out of L available diversity paths and combines them according to maximal ratio combining. PRAKE is not necessarily the best but it can reduce receiver complexity [14]. A traditional RAKE receiver employs the weighs vector $\boldsymbol{\beta} = \boldsymbol{\alpha}$ to realize MRC which maximizes the receiver output signal to noise ratio (SNR) when no interference is added to the system [15]. Therefore, the RAKE output can be expressed as

$$y(t) = \boldsymbol{\beta}^T \mathbf{r} = \sum_{l=0}^{L_p-1} \beta_l r_l(t). \tag{8}$$

C. IEEE 802.11a Systems Model

As most likely co-exist systems with UWB in the future, IEEE 802.11a systems operate around 5.2 GHz and overlap the band of UWB signals regulated by the FCC so that they will bring significant interference to UWB systems. These systems employ unlicensed national information infrastructure (U-NII) frequency bands using orthogonal frequency division multiplexing (OFDM) based transmission. In this spectrum there are three 100 MHz wide frequency bands which are 5.15~5.25 GHz, 5.25~5.35 GHz, and 5.725~5.825 GHz. An IEEE 802.11a system has 52 subcarriers each of which has the bandwidth of 16.6 MHz. It has been demonstrated that when the number of subcarriers is large enough a complex baseband OFDM signal can be modeled as bandlimited additive white Gaussian process [11]. With 52 subcarriers, IEEE 802.11a signals satisfy the condition and can be modeled as bandlimited additive white

Gaussian noise with PSD N_B. In [12], the author has demonstrated empirically that under the assumptions of the flat spectrum of such interference, to ignore the sidelobes of the spectrum, it is valid to model the IEEE 802.11a signals as bandlimited additive white Gaussian noise. In this paper, the worst situation is considered that means IEEE 802.11a signals occupy the full 300 MHz bandwidth. This may not be the case in the real situation but gives the worst performance in UWB systems.

III. NBI SUPPRESSION TECHNIQUE

In this section, we first review the classical singular value decomposition algorithm then develop our NBI suppression method.

SVD plays an important role in signal processing because it can split a signal space into a desired space and an unwanted one. For a time series $r(n)$ with $n = 1, 2, \cdots, N$, commonly, we can construct a Hankel matrix with $M = N - L + 1$ rows and L columns illustrated as follows

$$\mathbf{R} = \begin{bmatrix} r(1) & r(2) & \cdots & r(L) \\ r(2) & r(3) & \cdots & r(L+1) \\ \vdots & \vdots & & \vdots \\ r(N-L+1) & r(N-L+2) & \cdots & r(N) \end{bmatrix}, \quad (9)$$

then, $\mathbf{R}$ is an $M \times L$ matrix. Its elements can be found by substitution of $r(n)$

$$R_{ml} = r(m+l-1), m = 1, 2, \cdots, M \text{ and } l = 1, 2, \cdots, L. \quad (10)$$

Using SVD, $\mathbf{R}$ can be factorized as

$$\mathbf{R} = \mathbf{U}\mathbf{\Sigma}\mathbf{V}^H \quad (11)$$

where $\mathbf{U}$ and $\mathbf{V}$ are an $M \times M$ and $L \times L$ unitary matries. The columns of $\mathbf{U}$ and $\mathbf{V}$ are called left and right singular vectors, respectively. $\mathbf{\Sigma} = \text{diag}(\sigma_1, \sigma_2, \cdots, \sigma_m)$ is a diagonal matrix whose nonnegative entries are the square roots of the positive eigenvalues of $\mathbf{R}^H\mathbf{R}$ or $\mathbf{R}\mathbf{R}^H$. These nonnegative entries are called the singular values of $\mathbf{R}$ and they are arranged in a decreasing order with the largest one in the upper left-hand corner. $[\cdot]^H$ denotes the complex transpose of a matrix.

With the characteristic of white noise, the UWB signal has similar singular values which are all close to zero in the absence of high-energy NBI. After large NBI is introduced into the UWB system, there will exist several dominant singular values to represent such interference. In this case, the data matrix $\mathbf{R}$ is the superposition of the UWB signal space and the noise space and can be partitioned into two subspaces as follows:

$$\begin{aligned} \mathbf{R} &= \mathbf{U}\mathbf{\Sigma}\mathbf{V}^H \\ &= \begin{bmatrix} \mathbf{U}_R & \mathbf{U}_S \end{bmatrix} \begin{bmatrix} \mathbf{\Sigma}_R & 0 \\ 0 & \mathbf{\Sigma}_S \end{bmatrix} \begin{bmatrix} \mathbf{V}_R & \mathbf{V}_S \end{bmatrix}^H \\ &= \mathbf{U}_R\mathbf{\Sigma}_R\mathbf{V}_R^H + \mathbf{U}_S\mathbf{\Sigma}_S\mathbf{V}_S^H \\ &= \mathbf{R}_R + \mathbf{R}_S \end{aligned} \quad (12)$$

where

$$\mathbf{\Sigma}_R = \text{diag}(\sigma_1, \sigma_2, \cdots, \sigma_k) \quad (13)$$

and

$$\mathbf{\Sigma}_S = \text{diag}(\sigma_{k+1}, \sigma_{k+2}, \cdots, \sigma_m) \quad (14)$$

with $\sigma_1 > \sigma_2 > \cdots > \sigma_k \gg \sigma_{k+1} > \sigma_{k+2} > \cdots > \sigma_m$ corresponding to the singular values in the interference subspace and the data subspace, and $\sigma_1, \sigma_2, \cdots, \sigma_k$ are k dominant singular values. $\mathbf{R}_R = \mathbf{U}_R\mathbf{\Sigma}_R\mathbf{V}_R^H$ and $\mathbf{R}_S = \mathbf{U}_S\mathbf{\Sigma}_S\mathbf{V}_S^H$ are the interference subspace and the data subspace, respectively. Note that the computation of $\mathbf{R}_R$ can be realized by $\mathbf{R}_R = \mathbf{U}\hat{\mathbf{\Sigma}}\mathbf{V}^H$ where $\hat{\mathbf{\Sigma}}$ is obtained by setting to zero all but the k largest values in $\mathbf{\Sigma}$. By subtracting $\mathbf{R}_R$ from $\mathbf{R}$, we can get the estimated data matrix with suppressed NBI.

In summary, the SVD-based suppressing NBI consists of the following main steps:

1) Pick a number L so that $k < L < N - k$ [16], where k is the number of dominant singular values and N is the number of sampling points.
2) Arrange the received signal vector to form a Hankel data matrix $\mathbf{R}$ as (9).
3) Compute the SVD of $\mathbf{R}$ then obtain the estimated interference subspace $\mathbf{R}_R$.
4) Subtract $\mathbf{R}_R$ from $\mathbf{R}$ to get the estimated data matrix as

$$\tilde{\mathbf{R}}_S = \mathbf{R} - \mathbf{R}_R. \quad (15)$$

5) Rearrange the estimated matrix $\tilde{\mathbf{R}}_S$ into the vector and do performance detection in the receiver.

IV. NBI ALGORITHM PRECISION AND SYSTEM PERFORMANCE ANALYSIS

In order to investigate the effectiveness of our method, we will derive system performance and algorithm precision in this section.

A. System Performance Analysis

First, we define the UWB signal to NBI power ratio at the input of the receiver SIR_{in} as

$$\text{SIR}_{\text{in}} = P_{\text{UWB}}/P_R \quad (16)$$

and the UWB signal to AWGN power ratio SNR_{in} as

$$\text{SNR}_{\text{in}} = P_{\text{UWB}}/2\sigma^2 \quad (17)$$

where P_{UWB}, P_R, and σ^2, are respectively, the power of UWB signal, the power of NBI at the input of the receiver, and the variance of AWGN. By modeling IEEE 802.11a signals as bandlimited additive white Gaussian noise with PSD N_B, we can get $P_R = N_B W$, where W is the bandwidth of the NBI. In this paper, we consider NBI signal occupies the full 300 MHz bandwidth, that is to say $W = 300$ MHz.

Next, we will derive the SIR and SNR at the output of the receiver for the two UWB systems.

Substituting (3) and (5) into (7) gives

$$r_{\text{PAM}}^l(t) = d_i \sum_{j=0}^{N_s-1} \int_{(j-1)T_f}^{jT_f} \left\{ \sum_{l=0}^{L_p-1} \alpha_l w_{rx}(t - jT_f - \right.$$

$$C_jT_c-\tau_l)w_{rx}(t-jT_f-C_jT_c-\tau_l)\Big\}dt$$
$$+\sum_{j=0}^{N_s-1}\int_{(j-1)T_f}^{jT_f} i(t)w_{rx}(t-jT_f-C_jT_c-\tau_l)dt$$
$$+\sum_{j=0}^{N_s-1}\int_{(j-1)T_f}^{jT_f} n(t)w_{rx}(t-jT_f-C_jT_c-\tau_l)dt$$
$$=z^l_{\mathrm{PAM}}(t)+i^l_{\mathrm{PAM}}(t)+n^l_{\mathrm{PAM}}(t) \quad (18)$$

where

$$z^l_{\mathrm{PAM}}(t) = N_sd_i\alpha_l\int_{(j-1)T_f}^{jT_f} w^2_{rx}(t)dt = N_sd_i\alpha_lE_w, \quad (19)$$

$$i^l_{\mathrm{PAM}}(t)=\sum_{j=0}^{N_s-1}\int_{(j-1)T_f}^{jT_f} i(t)w_{rx}(t-jT_f-C_jT_c-\tau_l)dt \quad (20)$$

and

$$n^l_{\mathrm{PAM}}(t)=\sum_{j=0}^{N_s-1}\int_{(j-1)T_f}^{jT_f} n(t)w_{rx}(t-jT_f-C_jT_c-\tau_l)dt \quad (21)$$

correspond to the desired UWB signals, NBI, and AWGN contributions at the output of the lth correlator, respectively. $n^l_{\mathrm{PAM}}(t)$ is a Gaussian random variable with mean zero and variance $\frac{E_wN_0N_s}{2}$ with $E_w=\int_{(j-1)T_f}^{jT_f} w^2_{rx}(t)dt$.

Therefore we can obtain the output of the MRC PRAKE receiver with L_p fingers as

$$y_{\mathrm{PAM}}(t) = \sum_{l=0}^{L_p-1}\beta_l(z^l_{\mathrm{PAM}}(t)+i^l_{\mathrm{PAM}}(t)+n^l_{\mathrm{PAM}}(t)) = \boldsymbol{\beta}^T(\mathbf{z}_{\mathrm{PAM}}+\mathbf{i}_{\mathrm{PAM}}+\mathbf{n}_{\mathrm{PAM}}) \quad (22)$$

where $\mathbf{z}_{\mathrm{PAM}}=N_sd_iE_w\boldsymbol{\beta}$, $\mathbf{i}_{\mathrm{PAM}}=[i^0_{\mathrm{PAM}},i^1_{\mathrm{PAM}},\cdots,i^{L_p-1}_{\mathrm{PAM}}]^T$ and $\mathbf{n}_{\mathrm{PAM}}=[n^0_{\mathrm{PAM}},n^1_{\mathrm{PAM}},\cdots,n^{L_p-1}_{\mathrm{PAM}}]^T$ are the UWB signal, NBI, and AWGN components, respectively.

The resulting SIR and SNR can be given by

$$\mathrm{SIR}_{\mathrm{PAM}}=\frac{|\boldsymbol{\beta}^T\mathbf{z}_{\mathrm{PAM}}|^2}{E\{|\boldsymbol{\beta}^T\mathbf{i}_{\mathrm{PAM}}|^2\}}=\frac{(N_sE_w)^2|\boldsymbol{\beta}^T\boldsymbol{\beta}|^2}{\boldsymbol{\beta}^T\mathbf{R}^i_{\mathrm{PAM}}\boldsymbol{\beta}} \quad (23)$$

and

$$\mathrm{SNR}_{\mathrm{PAM}}=\frac{|\boldsymbol{\beta}^T\mathbf{z}_{\mathrm{PAM}}|^2}{E\{|\boldsymbol{\beta}^T\mathbf{n}_{\mathrm{PAM}}|^2\}}=\frac{(N_sE_w)^2|\boldsymbol{\beta}^T\boldsymbol{\beta}|^2}{\boldsymbol{\beta}^T\mathbf{R}^n_{\mathrm{PAM}}\boldsymbol{\beta}} \quad (24)$$

where $\mathbf{R}^i_{\mathrm{PAM}}=E\{\mathbf{i}_{\mathrm{PAM}}\mathbf{i}^H_{\mathrm{PAM}}\}$, $\mathbf{R}^n_{\mathrm{PAM}}=E\{\mathbf{n}_{\mathrm{PAM}}\mathbf{n}^H_{\mathrm{PAM}}\}$ are the correlation matrix of NBI and AWGN, respectively. Denote signal to interference and noise ratio (SINR) by

$$\mathrm{SINR}_{\mathrm{PAM}}=\frac{(N_sE_w)^2|\boldsymbol{\beta}^T\boldsymbol{\beta}|^2}{\boldsymbol{\beta}^T\mathbf{R}^i_{\mathrm{PAM}}\boldsymbol{\beta}+\boldsymbol{\beta}^T\mathbf{R}^n_{\mathrm{PAM}}\boldsymbol{\beta}}, \quad (25)$$

BER is approximated as [17]

$$P^b_{\mathrm{PAM}}=Q\left(\sqrt{2\mathrm{SINR}}\right)=Q\left(\sqrt{\frac{2(N_sE_w)^2|\boldsymbol{\beta}^T\boldsymbol{\beta}|^2}{\boldsymbol{\beta}^T\mathbf{R}^i_{\mathrm{PAM}}\boldsymbol{\beta}+\boldsymbol{\beta}^T\mathbf{R}^n_{\mathrm{PAM}}\boldsymbol{\beta}}}\right). \quad (26)$$

Another, for TH-BPPM UWB systems, substituting (4) and (6) into (7) and following the similar steps yields

$$r^l_{\mathrm{PPM}}(t) = \sum_{j=0}^{N_s-1}\int_{(j-1)T_f}^{jT_f}\Big\{\sum_{l=0}^{L_p-1}\alpha_lw_{rx}(t-jT_f-C_jT_c-\delta d_i-\tau_l)\times\Delta_{\mathrm{PPM}}(\delta d_i)\Big\}dt + \sum_{j=0}^{N_s-1}\int_{(j-1)T_f}^{jT_f} i(t)\times\Delta_{\mathrm{PPM}}(\delta d_i)dt + \sum_{j=0}^{N_s-1}\int_{(j-1)T_f}^{jT_f} n(t)\times\Delta_{\mathrm{PPM}}(\delta d_i)dt = z^l_{\mathrm{PPM}}(t)+i^l_{\mathrm{PPM}}(t)+n^l_{\mathrm{PPM}}(t) \quad (27)$$

where

$$z^l_{\mathrm{PPM}}(t) = (1-2d_i)N_s\alpha_l\int_{-\infty}^{+\infty} w_{rx}(t)[w_{rx}(t)-w_{rx}(t-\delta)]dt=(1-2d_i)N_s\alpha_lm_p, \quad (28)$$

$$i^l_{\mathrm{PPM}}(t)=\sum_{j=0}^{N_s-1}\int_{(j-1)T_f}^{jT_f} i(t)\Delta_{\mathrm{PPM}}(\delta d_i), \quad (29)$$

and

$$n^l_{\mathrm{PPM}}(t)=\sum_{j=0}^{N_s-1}\int_{(j-1)T_f}^{jT_f} n(t)\Delta_{\mathrm{PPM}}(\delta d_i). \quad (30)$$

Where $\Delta_{\mathrm{PPM}}(\delta d_i) = w_{rx}(t-jT_f-C_jT_c-\tau_l)-w_{rx}(t-jT_f-C_jT_c-\delta d_i-\tau_l)$ and $n^l_{\mathrm{PPM}}(t)$ is a Gaussian random variable with mean zero and variance $E_wN_0N_s$ with $E_w=\int_{(j-1)T_f}^{jT_f} w^2_{rx}(t)dt$.

Thus, we can obtain SIR, SNR, and approximate BER at the output of the MRC PRAKE receiver as [17]

$$\mathrm{SIR}_{\mathrm{PPM}}=\frac{|\boldsymbol{\beta}^T\mathbf{z}_{\mathrm{PPM}}|^2}{E\{|\boldsymbol{\beta}^T\mathbf{i}_{\mathrm{PPM}}|^2\}}=\frac{(N_sm_p)^2|\boldsymbol{\beta}^T\boldsymbol{\beta}|^2}{\boldsymbol{\beta}^T\mathbf{R}^i_{\mathrm{PPM}}\boldsymbol{\beta}}, \quad (31)$$

$$\mathrm{SNR}_{\mathrm{PPM}}=\frac{|\boldsymbol{\beta}^T\mathbf{z}_{\mathrm{PPM}}|^2}{E\{|\boldsymbol{\beta}^T\mathbf{n}_{\mathrm{PPM}}|^2\}}=\frac{(N_sm_p)^2|\boldsymbol{\beta}^T\boldsymbol{\beta}|^2}{\boldsymbol{\beta}^T\mathbf{R}^n_{\mathrm{PPM}}\boldsymbol{\beta}}, \quad (32)$$

and

$$P^b_{\mathrm{PPM}}=Q(\sqrt{\mathrm{SINR}})=Q(\sqrt{\frac{(N_sm_p)^2|\boldsymbol{\beta}^T\boldsymbol{\beta}|^2}{\boldsymbol{\beta}^T\mathbf{R}^i_{\mathrm{PPM}}\boldsymbol{\beta}+\boldsymbol{\beta}^T\mathbf{R}^n_{\mathrm{PPM}}\boldsymbol{\beta}}}) \quad (33)$$

where $\mathbf{z}_{\mathrm{PPM}}=(1-2d_i)N_sm_p\boldsymbol{\beta}$, $\mathbf{i}_{\mathrm{PPM}}=[i^0_{\mathrm{PPM}},i^1_{\mathrm{PPM}},\cdots,i^{L_p-1}_{\mathrm{PPM}}]^T$ and $\mathbf{n}_{\mathrm{PPM}}=[n^0_{\mathrm{PPM}},n^1_{\mathrm{PPM}},\cdots,n^{L_p-1}_{\mathrm{PPM}}]^T$ correspond to the desired UWB signal, NBI, and AWGN components, respectively. $\mathbf{R}^i_{\mathrm{PPM}}=E\{\mathbf{i}_{\mathrm{PPM}}\mathbf{i}^H_{\mathrm{PPM}}\}$ and $\mathbf{R}^n_{\mathrm{PPM}}=$

$E\{\mathbf{n}_{\mathrm{PPM}}\mathbf{n}_{\mathrm{PPM}}^H\}$ are the correlation matrix of NBI and AWGN, respectively.

B. SVD Algorithm Performance

In this section, SVD algorithm performance will be derived. Let $\mathbf{R}_S = \mathbf{U}_S\mathbf{\Sigma}_S\mathbf{V}_S^H$ be the SVD of the received data matrix in the absence of NBI and $\tilde{\mathbf{R}}_S = \tilde{\mathbf{U}}_S\tilde{\mathbf{\Sigma}}_S\tilde{\mathbf{V}}_S^H$ be the SVD of the received data matrix with NBI suppressed by using our method. We can observe that $\tilde{\mathbf{\Sigma}}_S$ is obtained by substituting zeros for the k dominant singular values in the diagonal matrix in (12). So the mean-squared error (MSE) in this approximation is

$$\delta_{\mathrm{SVD}}^2 = \|\mathbf{R}_S - \tilde{\mathbf{R}}_S\|^2 = \mathrm{trace}\left[(\mathbf{R}_S - \tilde{\mathbf{R}}_S)(\mathbf{R}_S - \tilde{\mathbf{R}}_S)^H\right]. \quad (34)$$

Simple calculation yields the estimation precision which has the form as

$$\begin{aligned}\delta_{\mathrm{SVD}}^2 = \mathrm{trace}[&\mathbf{U}_S\mathbf{\Sigma}_S^2\mathbf{U}_S^H - \mathbf{U}_S\mathbf{\Sigma}_S\mathbf{V}_S^H\tilde{\mathbf{V}}_S\tilde{\mathbf{\Sigma}}_S\tilde{\mathbf{U}}_S^H \\ &-\tilde{\mathbf{U}}_S\tilde{\mathbf{\Sigma}}_S\tilde{\mathbf{V}}_S^H\mathbf{V}_S\mathbf{\Sigma}_S\mathbf{U}_S^H + \tilde{\mathbf{U}}_S\tilde{\mathbf{\Sigma}}_S^2\tilde{\mathbf{U}}_S^H].\end{aligned} \quad (35)$$

On the assumption that $\mathbf{U}_S \approx \tilde{\mathbf{U}}_S$ and $\mathbf{V}_S \approx \tilde{\mathbf{V}}_S$, the performance of SVD can be approximated by

$$\delta_{\mathrm{SVD}}^2 \approx \sum_{i=1}^{k}\sigma_i^2 < k\sigma_{\max}^2 \quad (36)$$

where σ_i is the singular value of the signal matrix $\mathbf{R}_S$ when no NBI is added into the system and $\sigma_{\max}$ is the maximum one among them. With the small $\sigma_{\max}$ (close to zero), we can observe that the the maximum variance δ_{SVD}^2 is trivial so that good suppression effectiveness can be obtained by using SVD algorithm. Also, from the above analysis we can observe that the estimated data matrix $\tilde{\mathbf{R}}_S$ is the best least squares approximation of lower rank to the given data matrix $\mathbf{R}_S$.

C. Calculation Complexity Analysis

In this part, we will compare the calculation complexity of the proposed SVD-based approach and the traditional multi-fingers RAKE receiver. For the proposed approach the complexity depends on the SVD algorithm. Only thinking about the complex multiplication and by using the sliding window adaptive SVD technique [18], the calculation complexity can be obtained by

$$\begin{aligned}\mathrm{Complexity}_{\mathrm{SVD}} = &\ 8Lk + 8Nk + 10N + 4k^2 + 24k^3 \\ &+8Nk^2 + LMk + Mk\end{aligned} \quad (37)$$

while by ignoring the channel estimation complexity, the complexity of the multi-fingers RAKE receiver can be expressed by

$$\mathrm{Complexity}_{\mathrm{RAKE}} = L_a(N+4) \quad (38)$$

where N is the number of sampling points and L_a is the number of RAKE fingers. Usually, L and M have a linear relationship with N, so we can observe from (37) that the complexity of the proposed SVD-based method has the quadric relationship with N. However, we can not say the proposed method has a higher complexity. Actually, when the NBI is strong, the required L_a is very high (usually several hundred) to obtain the target performance [14]. In the extreme case, for a very strong NBI, the traditional method will be completely infeasible to suppress such NBI while the proposed method can still work very well. Furthermore, a several-hundred fingers RAKE receiver is limited to be utilized by the current channel estimation techniques [14].

V. SIMULATION RESULTS AND DISCUSSION

A. Simulation Parameters

At the transmitter, the second-derivative Gaussian pulse is used as the transmitted UWB monocycle [19] and the transmitted signal is modulated as $N_p = 24$, $T_p = 1$ ns, $T_c = 2$ ns, $T_f = 50$ ns, and $\delta = 1$ ns for TH-BPAM and TH-BPPM UWB signals. The adopted channel model is the IEEE UWB multipath channel model according to [20]. In order to avoid introducing much multipath interference, the CM1 model with parameters $(\Lambda, \lambda, \Gamma, \gamma) = (0.0233\ \mathrm{ns}^{-1}, 2.5\ \mathrm{ns}^{-1}, 7.1\ \mathrm{ns}, 4.3\ \mathrm{ns})$ for an indoor channel with line of sight (LOS) is used. According to the analysis in Section II, IEEE 802.11a signals are modeled as bandlimited additive white Gaussian noise with bandwidth 300 MHz. Note that in the rest of the paper, when SVD algorithm is used, the receiver is a 3-fingers MRC PRAKE receiver and we pick $L = N/5$ to satisfy $k < L < N - k$. We consider the $\mathrm{SIR}_{\mathrm{in}} = -20$ dB and -30 dB. Thinking of the high PSD of IEEE 802.11a signals with respect to that of UWB signals, we think this interference level feasible.

It has been shown in [16], [21] that when the column number L in a Hankel matrix satisfies the inequality $k < L < N - k$, we can obtain the correct or approximately correct estimation result. However, to the best of our knowledge, it has not been seen that the optimal L theoretically, moreover, the optimal L is different in different cases. Some researchers gave suggestions in several applications by simulations and experience [21]–[24]. In [22], the optimal value of L is proposed as

$$L = \begin{cases}(N+1)/2, & N = 1, 3, 5, \cdots, \\ N/2, & N = 2, 4, 6, \cdots.\end{cases} \quad (39)$$

In [21], L is recommended to be approximately $L = N/3$ for a best frequency estimation.

In our work, the simulation results show that L decides the size of the Hankel matrix so that it determines the computation complexity and the number of dominant singular values. Satisfying $k < L < N - k$, different L has no significant impact on the system performance. On the other hand, with more computational complexity and worse performance, $L = N/2$ is not an optimal choice. Therefore, considering running efficiency and better performance, the suggested L is normally between $N/5$ and $N/3$.

B. Simulation Results

We assume that the receiver synchronizes to the desired signal, in this section the simulation results will be presented. Fig. 1 shows the BER performance versus $\mathrm{SNR}_{\mathrm{in}}$ for a MRC PRAKE receiver with 3, 8, and 10 fingers in TH-BPAM UWB systems. From this figure, we can observe that a MRC PRAKE

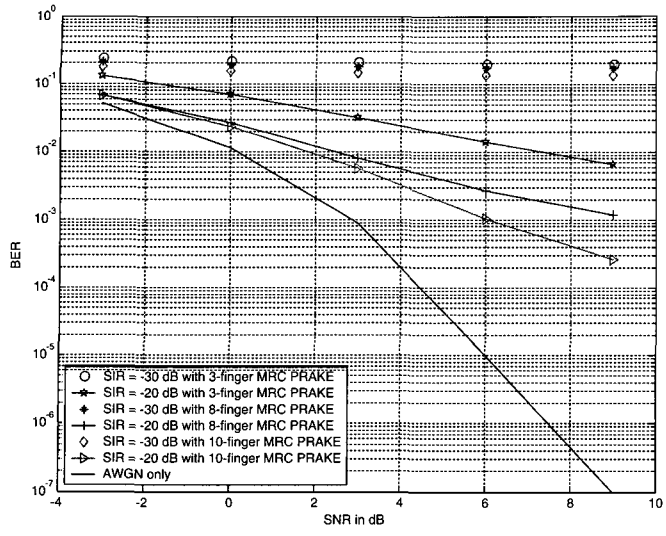

Fig. 1. NBI suppressing using MRC PRAKE with different fingers in TH-BPAM UWB systems.

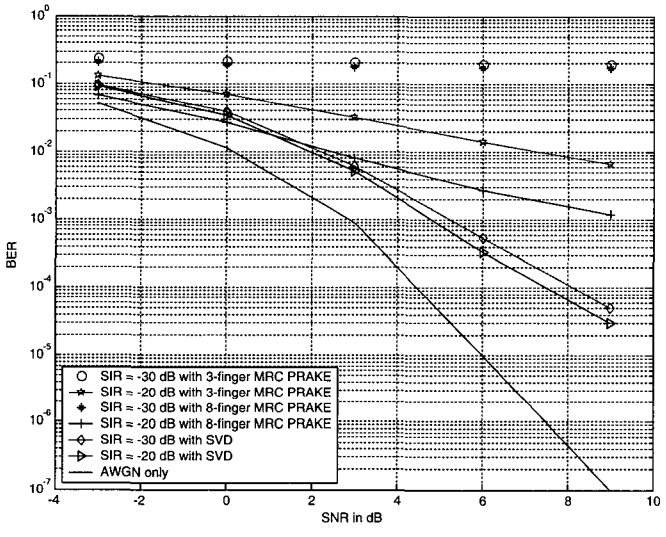

Fig. 2. NBI suppressing using SVD and multi-fingers MRC PRAKE receiver in TH-BPAM UWB systems.

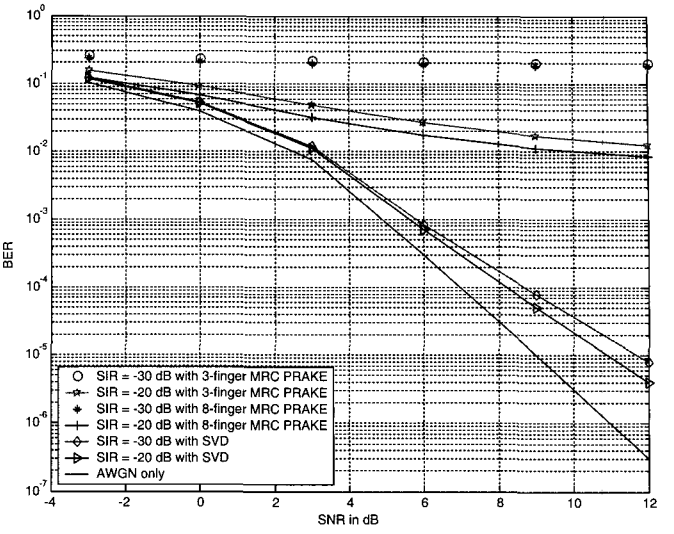

Fig. 3. NBI suppressing using SVD and multi-fingers MRC PRAKE receiver in TH-BPPM UWB systems.

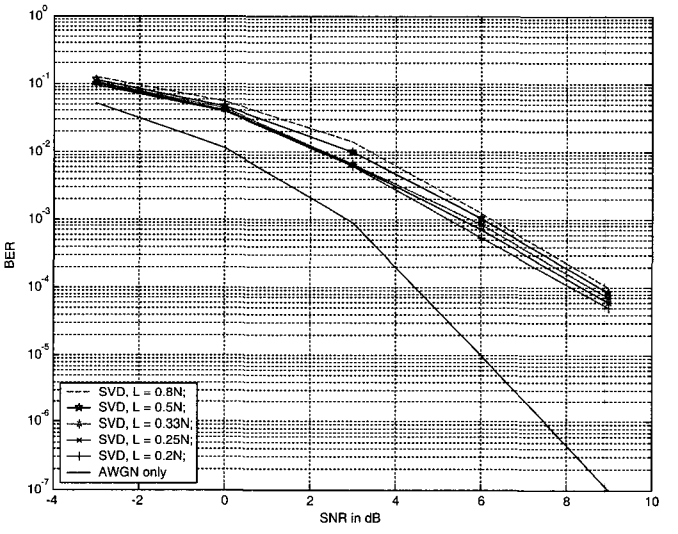

Fig. 4. NBI suppressing using SVD with different L in TH-BPAM UWB systems.

is jammed even when the number of fingers is 10. This proves the importance of suppressing NBI, and thus, combating this performance degradation. Figs. 2 and 3 present the effectiveness of our approach to suppress IEEE 802.11a interference both in TH-BPAM and TH-BPPM UWB systems. By comparing with a 3-fingers MRC PRAKE and an 8-fingers MRC PRAKE, we can conclude that the NBI is mitigated greatly by using our technique and system performance is improved very effectively. For instance, in a TH-BPAM system, for the desired BER of 10^{-3} and when $\mathrm{SIR}_{\mathrm{in}} = -20$ dB, the SVD-based method can get over 4 dB improvement than an 8-fingers MRC PRAKE receiver. From this figure, we can observe that by using the proposed method only a 3-fingers RAKE receiver is enough to suppress such strong NBI. Since the hardware complexity of the RAKE receiver depends on the number of RAKE fingers, our approach can reduce the hardware complexity of the receiver greatly.

To study the robustness of our algorithm, we compare the results of the SVD-based method under different L in TH-BPAM systems when $\mathrm{SIR}_{\mathrm{in}} = -30$ dB. Fig. 4 plots the simulation results when $L = N/5, N/4, N/3, N/2$, and $4N/5$, respectively. In this case, although we take different L, our algorithm can still mitigate the NBI effectively with slight difference. Actually, satisfying $k < L < N - k$, L decides the number of dominant singular values representing the NBI and computation amount of the suppression technique and has no significant impact on system performance. So, considering running efficiency and system performance, the optimal L is recommended by between $L = N/5$ and $L = N/3$. From the figure, we can observe that as the decrease of L, better system performance can be attained. This is because that L decides the number of the dominant singular values k, when L is reduced, k is also reduced correspondingly. According to (36), we know the system performance is improved. However, it is not to say the less the L is, the better the results are. In fact, when L is too small, replacing the dominant singular values by zeros introduces much error so that the approximation (36) is not feasible.

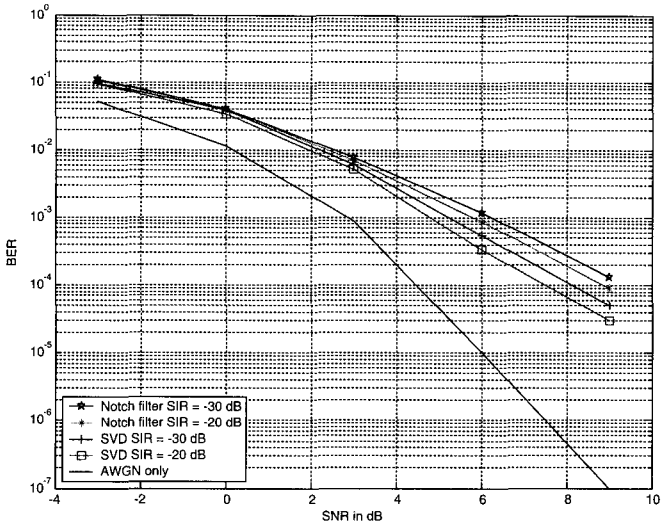

Fig. 5. NBI suppressing using SVD and notch filter in TH-BPAM UWB systems.

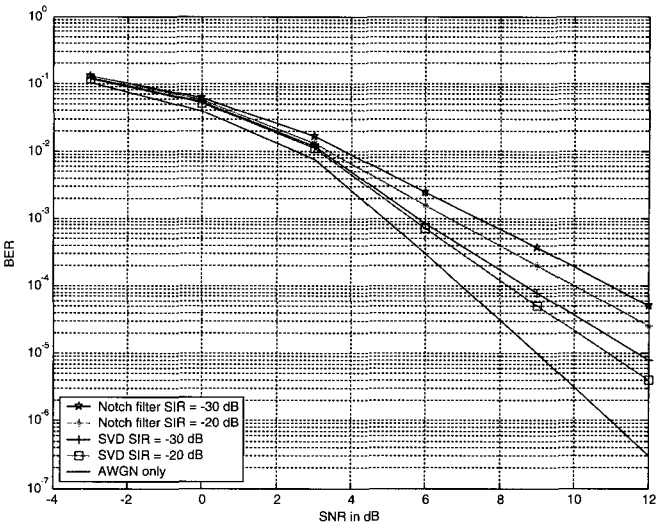

Fig. 6. NBI suppressing using SVD and notch filter in TH-BPPM UWB systems.

To investigate the effectiveness of our method, we compare the performance of our method with the conventional methods, such as a notch filter in Figs. 5 and 6 in both TH-BPAM and TH-BPPM UWB systems. The notch filter is a Chebyshev II-based IIR bandstop filter with passband ripple 1 dB and stopband attenuation 40 dB. Chebyshev II type filter presents better performance than other conventional filters when it is used to be a prototype filter in designing a notch filter [25]. From the two figures we can observe clearly that by using our method, we can obtain better performance than by using a notch filter. For example, in TH-BPPM systems, when $\mathrm{SIR}_{\mathrm{in}} = -30$ dB and at the target BER of 10^{-4}, our algorithm can obtain over 2 dB improvement than the conventional method. Unlike our method, the center frequency of the narrow-band interference need to be estimated and the center frequency of the notch filter need to be adjustable to meet the specific NBI. Furthermore, such in-band notches may impair the performance of UWB signals simultaneously [15]. Hence, as the increase of NBI bandwidth, our method can achieve better performance than a notch filter.

VI. CONCLUSION

A novel SVD-based algorithm to suppress IEEE 802.11a interference in TH-UWB systems is proposed. The analysis and simulation results show that singular value decomposition of the data matrix is very useful in finding the dominant singular values corresponding to the narrow-band interference and to obtain the estimated data matrix. By comparing with the other traditional NBI suppression methods, it is concluded that our algorithm is very effective to suppress IEEE 802.11a signals in TH-UWB systems and the complexity of the receiver can be reduced dramatically. Our method is simple and robust and especially suitable for UWB systems.

REFERENCES

[1] "Revision of part 15 the Commission's rules regarding ultra-wideband transmission systems," FCC, ET Docket, pp. 98–153, Apr. 2002.

[2] M. Hämälainen, R. Tesi, and J. Iinatti, "On the UWB system coexistence with GSM900, UMTS/WCDMA, and GPS," *IEEE J. Sel. Areas Commun. Special Issue on UWB*, vol. 20, pp. 1712–721, Dec. 2002.

[3] J. R. Foerster, "The performance of a direct-sequence spread ultra wideband system in the presence of multipath, narrowband interference and multiuser interference," in *Proc. IEEE Conf. Ultra Wideband Syst. Technol.*, 2002, pp. 87–92.

[4] I. Bergel, E. Fishler, and H. Messer, "Narrow-band interference suppression in time-hopping impulse-radio systems," in *Proc. IEEE Conf. Ultra Wideband Syst. Technol.*, 2002, pp. 303–308.

[5] N. Boubaker and K. B. Letaief, "Low complexity MMSE-RAKE receiver in a realistic UWB channel and in the presence of NBI," in *Proc. IEEE WCNC*, vol. 1, 2003, pp. 233–237.

[6] E. Baccarelli, M. Biagi, and L. Taglione, "A novel approach to in-band interference mitigation in ultra wideband radio systems," in *Proc. IEEE Conf. Ultra Wideband Syst. Technol.*, Digest of Papers 2002, pp. 297–301.

[7] L. Li and L. Milstein, "Rejection of narrow-band interference in pn spread spectrum systems using transversal filters," *IEEE Trans. Commun.*, vol. 30, no. 9, pp. 925–928, 1982.

[8] V. Bharadwaj and R. M. Buehrer, "An interference suppression scheme for UWB signals using multiple receive antennas," *IEEE Commun. Lett.*, vol. 9, pp. 529–531, Jun. 2005.

[9] A. Taha and K. M. Chugg, "A theoretical study on the effects of interference on UWB multiple-access impulse radio," in *Proc. ACSSC*, vol.1, Nov. 2002, pp. 728–732.

[10] V. Gonzalez and W. A. Moreno, "Narrowband interference detection in multiband UWB systems," in *Proc. IEEE/Sarnoff Symposium on Advances in Wired and Wireless Communication*, Apr. 2005, pp. 160–163.

[11] Q. Li and L. A. Rusch, "Multiuser detection for DS-CDMA UWB in the home environment," *IEEE J. Sel. Areas Commun.*, vol. 20, pp. 1701–1711, Dec. 2002.

[12] B. Firoozbakhsh, T. G. Pratt, and N. Jayant, "Analysis of IEEE 802.11a interference on UWB systems," in *Proc. IEEE Conf. Ultra Wideband Syst. Technol.*, Nov. 2003, pp. 473–477.

[13] S. Y. Xu, Z. Q. Bai, Q. H. Yang, and K. S. Kwak, "Singular value decomposition-based algorithm for IEEE 802.11a interference suppression in DS-UWB systems," *IEICE Trans. Fundament.*, no. 7, pp. 1913–1918, 2006.

[14] D. Cassioli, M. Z. Win, F. Vatalaro, and A. F. Molisch, "Performance of low-complexity rake reception in a realistic UWB channel," in *Proc. IEEE ICC*, New York, USA, vol. 2, Apr. 2002, pp. 763–767.

[15] X. Chu and R. D. Murch, "The effect of NBI on UWB time-hopping systems," *IEEE Trans. Wireless Commun.*, vol. 3, pp. 1431–1436, Sept. 2004.

[16] K. C. Teh, C. C. Teng, A. C. Kot, and K. H. Li, "Jammer suppression in spread spectrum," in *Proc. IEEE Conf. Inf. Eng.*, 1995, pp. 220–224.

[17] M. G. D. Benedetto and G. Giancola, *Understanding Ultra Wide Band Radio Fundamentals*. Prentice Hall PTR, 2004.

[18] R. Badeau, G. Richard, and B. David, "Sliding window adaptive SVD algorithms," *IEEE Trans. Signal Process.*, vol. 52, pp. 1–10, Jan. 2004.

[19] M. Z. Win and R. A. Scholtz, "Ultra-wide bandwidth time-hopping spread-

spectrum impulse radio for wireless multiple-access communications," *IEEE Trans. Commun.*, vol. 48, pp. 679–689, Apr. 2000.

[20] IEEE P802.15 Working Group for WPAN, "Channel modeling subcommittee report final," IEEE P802.15-02/368rSG3a, Nov. 2002.

[21] D. Tufts and R. Kumaresan, "Singular value decomposition and improved frequency estimation using linear prediction," *IEEE Trans. Acoust., Speech, and Signal Process.*, vol. 30, no. 4, pp. 671–675, Aug. 1982.

[22] B. Hu and R. G. Gosine, "A new eigenstructure method for sinusoidal signal retrieval in white noise: Estimation and pattern recognition," *IEEE Trans. Signal Process.*, vol. 45, no. 12, pp. 3073–3083, Dec.1997.

[23] Y. Hua and T. K. Sarkar, "On SVD for estimating generalized eigenvalues of singular matrix pencil in noise," *IEEE Trans. Signal Process.*, vol. 39, no. 4, pp. 892–899, Apr. 1991.

[24] P. Stoica, Y. Selen, N. Sandgren, and S. V. Huffel, "Using prior knowledge in SVD-based parameter estimation for magnitic resonance spectroscopy–The ATP example," *IEEE Trans. Biomed. Eng.*, vol. 51, no. 9, pp. 1568–1578, Sept. 2004.

[25] D. Economou, C. Mavroidis, and I. Antoniadis, "Comparison of filter types used for command preconditioning in vibration suppression applications," in *Proc. American Control Conf. 2002*, vol. 3, May, 2002, pp. 2273–2278.

Shaoyi Xu received the B.S. and M.S. degrees from Shenyang Institute Aeronautical Engineering in 1997 and China Agricultural University in 2000, respectively. In August 2007, she received her Ph.D. degree in the Graduate School of Information Technology and Telecommunications, Inha University, Korea. She has research interests in narrowband interference (NBI) suppression, multi-access interference (MAI) suppression, and intersymbol interference (ISI) suppression for UWB communication systems. From September 2007 to now, she works in Nokia Research Center in Beijing, China as a postdoctor. Her research is focusing on the cooperative MIMO communications and cognitive radio networks.

Kyung Sup Kwak received the B.S. degree from the Inha University, Incheon, Korea in 1977, the M.S. degree from the University of Southern California in 1981, and the Ph.D. degree from the University of California at San Diego in 1988, under the Inha University Fellowship and the Korea Electric Association Abroad Scholarship Grants, respectively. From 1988 to 1989, he was a member of technical staff at Hughes Network Systems, San Diego, California. From 1989 to 1990, he was with the IBM Network Analysis Center at Research Triangle Park, North Carolina. Since then, he has been with the School of Information and Communication, Inha University, Korea as a professor.

He had been the chairman of the School of Electrical and Computer Engineering from 1999 to 2000 and the dean of the Graduate School of Information Technology and Telecommunications from 2001 to 2002 at the Inha University, Incheon, Korea. He is the current director of Advanced IT Research Center of Inha University, and UWB Wireless Communications Research Center, a key government IT research center, Korea.

Since 1994, he had been serving as a member of Board of Directors, and during the term of 2002–2000 year, he had been the vice president for Korean Institute of Communication Sciences (KICS). He has been elected for the KICS's president of 2006 year term. In 1993, he received Engineering College Young Investigator Achievement Award from Inha University, and a distinguished service medal from the Institute of Electronics Engineers of Korea (IEEK). In 1996 and 1999, he received distinguished service medals from the KICS. He received the Inha University Engineering Paper Award and the LG Paper Award in 1998, and Motorola Paper Award in 2000. His research interests include multiple access communication systems, mobile communication systems, UWB radio systems and ad-hoc networks, high-performance wireless Internet. He is members of IEEE, IEICE, KICS, and KIEE.